Published in final edited form as:
Biochemistry. 2010 March 9; 49(9): 1985–1997. doi:10.1021/bi902065k.

Identification of bZIP interaction partners of viral proteins HBZ, MEQ, BZLF1, and K-bZIP using coiled-coil arrays

Aaron W. Reinke, **Gevorg Grigoryan**, and **Amy E. Keating***
Department of Biology, Massachusetts Institute of Technology, Cambridge, MA 02139

Abstract

Basic-region leucine-zipper transcription factors (bZIPs) contain a segment rich in basic amino acids that can bind DNA, followed by a leucine zipper that can interact with other leucine zippers to form coiled-coil homo- or heterodimers. Several viruses encode proteins containing bZIP domains, including four that encode bZIPs lacking significant homology to any human protein. We investigated the interaction specificity of these four viral bZIPs by using coiled-coil arrays to assess self-associations as well as hetero-interactions with 33 representative human bZIPs. The arrays recapitulated reported viral-human interactions and also uncovered new associations. MEQ and HBZ interacted with multiple human partners and had unique interaction profiles compared to any human bZIPs, whereas K-bZIP and BZLF1 displayed homo-specificity. New interactions detected included HBZ with MAFB, MAFG, ATF2, CEBPG, and CREBZF, and MEQ with NFIL3. These were confirmed in solution using circular dichroism. HBZ can hetero-associate with MAFB and MAFG in the presence of MARE-site DNA, and this interaction is dependent on the basic region of HBZ. NFIL3 and MEQ have different yet overlapping DNA-binding specificities and can form a heterocomplex with DNA. Computational design considering both affinity for MEQ and specificity with respect to other undesired bZIP-type interactions was used to generate a MEQ dimerization inhibitor. This peptide, anti-MEQ, bound MEQ both stably and specifically, as assayed using coiled-coil arrays and circular dichroism in solution. Anti-MEQ also inhibited MEQ binding to DNA. These studies can guide further investigation of the function of viral and human bZIP complexes.

Many viruses hijack cellular machinery by using viral proteins to interact with host proteins. Viruses can incorporate host protein domains into their genomes for this purpose, as is the case for several viruses that use BCL-2 homologs to prevent apoptosis. Viral host-derived protein domains often make interactions similar to those of their homologues, although these can occur in a misregulated manner (1). Alternatively, host-derived protein domains can diverge from their cellular counterparts, such that they retain little sequence similarity. In such cases, virus-host protein interactions can be expected to differ markedly from corresponding host-host complexes (2).

The bZIP transcription factors are a large class of proteins found in most eukaryotic organisms. Named for their DNA-binding and dimerization domain, bZIP proteins interact with DNA site-specifically via a region of conserved basic amino acids. Immediately C-terminal to the basic region is the leucine zipper, a coiled coil that mediates the formation of homodimeric or heterodimeric complexes. The dimerization specificity of the leucine zippers allows for combinatorial interactions that can influence DNA binding and thus transcriptional regulation (3,4). Given the importance of protein partnering specificity for the function of the bZIPs, a

*To whom correspondence should be addressed. Telephone: 617-452-3398; Fax: 617-253-4043; keating@mit.edu.

Supporting Information **Available**: Sequences of protein used, comparison of human and chicken bZIPs sequences and additional coiled-coil array and gel-shift experiments. This material is available free of charge via the Internet at http://pubs.acs.org

high-throughput protein array assay was used to determine the global *in vitro* interaction profiles of most human bZIPs. The coiled-coil microarray assay used for this purpose was shown to identify most reported interactions, and the relative stabilities of interactions measured on the arrays were also shown to agree well with solution measurements (5,6).

Proteins containing bZIP domains have been identified in several viruses. Three human bZIP proteins, JUN (cJun), FOS (cFos), and MAF (cMaf), occur in an altered form in oncogenic avian and murine retroviruses. These homologous viral bZIPs maintain the protein dimerization properties of the human proteins and are oncogenic because of altered regulation (7-9). Four viral bZIPs that have little homology to human bZIPs have also been identified, and although several interactions with host proteins have been reported, global investigation of the interactions of these proteins with host bZIPs is lacking.

Human T-cell leukemia virus type 1 is a retrovirus that causes adult T-cell leukemia; it encodes the bZIP protein HBZ (reviewed in (10)). HBZ has been shown to repress both viral and cellular gene expression. A recent study suggests that in addition to the role of the HBZ protein in disease progression, the mRNA of HBZ promotes proliferation (11). Interactions have been reported between HBZ and many human bZIPs both *in vivo* and *in vitro* including ATF4, JUN, JUNB, JUND, CREB1, ATF1, and CREM (12-15). HBZ has been shown to form complexes with JUN, JUNB, CREB1, and ATF4 and to prevent these proteins from binding DNA. In contrast, HBZ has been reported to increase the transcriptional activity of JUND (13).

MEQ is encoded by Marek's disease virus (MDV), an oncogenic herpes virus that infects chickens. The disease is estimated to cost the US poultry industry one billion dollars annually (reviewed in (16)). MEQ has been demonstrated to be largely responsible for the oncogenic properties of MDV (17-19). MEQ can self-associate as well as interact with a variety of other bZIPs *in vitro* including: JUN, JUNB, CREB1, ATF1, ATF2, ATF3, FOS, and BATF3 (17, 20-22). Additionally, MEQ has been shown to bind JUN *in vivo*, and JUN is required for MEQ to transform cells (18,20).

Two gammaherpesviruses are reported to encode bZIP-containing proteins. These viruses are implicated in several proliferative disorders in humans. Epstein-Barr virus encodes BZLF1 (ZEBRA, Zta, Z, EB1) and is associated with Burkitt's lymphoma, Hodgkin's disease, and nasopharyngeal carcinoma. Kaposi's sarcoma-associated herpesvirus encodes K-bZIP (K8, RAP) and is involved in Kaposi's sarcoma, primary effusion lymphoma, and multicentric Castleman's disease (reviewed in (23,24)). These two proteins are positional homologs and also share low sequence similarity with one another (25). BZLF1 is responsible for triggering the switch from latent to lytic infection by binding sites within the viral genome and causing transcriptional activation of many genes. It is also involved in viral replication (26,27). Over-expression of K-bZIP does not cause virus reactivation, but K-bZIP is necessary for viral replication as well as the repression and activation of many genes within the viral genome, though not always through direct binding to promoters (28,29). BZLF1 and K-bZIP both interact with many viral and cellular proteins including the human bZIP CEBPA (C/EBPα) (30). Interestingly, the interaction with CEBPA for both BZLF1 and K-bZIP is proposed to involve higher order oligomers rather than just dimers (31,32). Recently, the crystal structure of BZLF1 was solved showing that a C-terminal region adjacent to the leucine zipper folds back and stabilizes the coiled-coil structure, significantly stabilizing the homodimer (33). K-bZIP has been shown to self associate through its leucine zipper, but this homomeric interaction was reported to be one of higher order oligomers (25,32).

Given the importance of both human and viral bZIPs to human health, several strategies have been used to generate inhibitors that can prevent dimerization and/or DNA binding. One approach is to use the leucine zipper of a homodimerizing bZIP as a dominant negative. The

utility of this approach has been demonstrated in the context of BZLF1. Using a peptide that consisted of only the leucine zipper of BZLF1, (34) Hicks et al. showed that BZLF1 could be prevented from binding DNA. However, the EC_{50} for the peptide was high micromolar. A possible disadvantage of using native leucine-zipper peptides as inhibitors is that these may associate with bZIPs other than the desired target. Recently, we reported a computational design method for obtaining peptides that interact specifically with leucine zippers and applied it to a range of human targets. Out of the 20 human bZIP families, peptides were designed that successfully interacted with 19. Of these 19, 8 designs bound to their target family stronger than to any other family (5).

Here we report all pair-wise interactions of four bZIP peptides derived from viral proteins with 33 human bZIP proteins measured using peptide microarrays. We identified several new interactions for both MEQ and HBZ, and these interactions were confirmed using circular dichroism and gel-shift assays. Additionally, we designed a peptide, anti-MEQ, to serve as a MEQ dimerization inhibitor. We demonstrate that this peptide binds specifically to MEQ and can prevent MEQ from binding DNA.

Experimental Methods

Plasmid construction, protein expression and purification

Human protein constructs used for array experiments have been previously described and are listed in Table S1 (5,6). Synthetic genes encoding the leucine zipper regions of HBZ, MEQ, BZLF1, K-bZIP, anti-MEQ and the full bZIP domains of MAFB, HBZ, and MEQ were synthesized using DNAWorks to design primers and a two-step PCR method to anneal them (35). The bZIP domains of CREBZF and ATF2 were cloned from plasmids acquired from Open Biosystems (36) and NFIL3, JUN, CEBPG and MAFG were cloned from plasmids obtained from PlasmID (37). These proteins were cloned into modified versions of a pDEST17 vector. Proteins were expressed in RP3098 cells and purified under denaturing conditions using Ni-NTA followed by reverse-phase HPLC as described previously (5,6). A tagless version of anti-MEQ used for gel-shift and CD studies was constructed by cloning into pSV282 (Vanderbilt University Medical Center, Center for Structural Biology). The 6XHIS-MBP-anti-MEQ fusion protein was expressed in RP3098 cells by growing a 1 L culture in LB at 37 °C and inducing at 0.5 OD by adding 1 mM IPTG and growing for 4 hours. The fusion protein was purified under native conditions by binding to Ni-NTA resin (Qiagen) and eluted by adding 8 ml buffer (300 mM imidazole, 20 mM TRIS, 500 mM NaCl, 1 mM DTT, pH 7.9). The fusion protein was then dialyzed overnight into TEV cleavage buffer (50 mM TRIS, 50 mM NaCl, 1 mM DTT, 0.5 mM EDTA, pH 7.5) and then cleaved by adding 100 μl TEV protease (1mg/ml) for 3 hours at 18-22 °C. This mixture was then added to Ni-NTA resin and the flow-through collected. The anti-MEQ peptide was further purified using reverse-phase HPLC. The molecular weights of the peptides were confirmed by mass spectrometry. Protein sequences generated for this study are listed in Table S1.

Coiled-coil arrays

Array experiments were performed as described previously (5). The average background-corrected fluorescence values for all measurements are listed in Table S2. Two measures used to report fluorescence intensities in the figures are S_{array} and *arrayscore*. These are defined in references (5) and (38), respectively. S_{array} was calculated using the equation

$$S_{array}(a)=\frac{(a-\tilde{a})}{\sqrt{\sum_{i=1,ai<\tilde{a}}^{N}(a_i-\tilde{a})^2/N_{a<\tilde{a}}}}$$

where a was the average fluorescence intensity of a protein on the surface and $\tilde{a}$ was the median signal for all proteins on the surface interacting with the

same solution probe, N was the number of proteins on the surface, and $N_{a<\tilde{a}}$ was the number of proteins with a value a below the median. The *arrayscore values* were calculated using the equation −log(F/Fmax) where F was the average fluorescence intensity of each protein on the surface minus the median signal for all proteins on the surface interacting with the same solution protein and Fmax was the maximum F.

Circular dichroism

Circular dichroism experiments were performed as described previously (5). ãThe concentrations used for each experiment are listed in the figure legends. Thermal dentaturations were measured from 0 to 65 °C and all were reversible with all complexes having differences in T_m of less than 3 °C upon refolding. The buffer for CD measurements of MEQ was PBS (12.5 mM potassium phosphate (pH 7.4) and 150 mM KCl) with 1mM DTT. For measurements of HBZ the buffer also included 200 mM GdnHCl and 0.25 mM EDTA.

Phylogenetic analysis

An unrooted phylogenetic tree was constructed using the neighbor-joining method for the 53 human and 4 viral bZIP leucine-zipper regions as described previously (5). For comparison of chicken and human sequences, each human bZIP was used to BLAST the *G. gallus* genome and 41 chicken bZIPs were identified. Leucine-zipper regions were defined as previously reported (6). Families were defined according to evolutionary conservation and interaction profiles, as in (6,39).

Gel-shift assay

DNA probes for the AP-1, TFIID, and NF-κB sites were obtained from Promega. Other probes were based on literature-defined sequences (MARE (40), CAAT (41), CRE1 (20), CRE2 (42), MDVORI (20)), ordered as PAGE-purified oligos (IDT) and then annealed. Probes were end labeled with [γ-^{32}P]ATP using PNK (NEB). Proteins were incubated for 3 hours at 18-22 °C in gel-shift buffer (50 mM KCl, 25 mM TRIS pH 8.0, 0.5 mM EDTA, 2.5 mM DTT, 1 mg/ml BSA, 10% (v/v) glycerol, 0.1 mg/ml competitor DNA (Poly (I)·Poly (C) (GE)). Radiolabeled DNA was then added and incubated for 1 hour at 18-22 °C. Radiolabeled DNA was at a final concentration of 0.7 nM, except for experiments in Figure S4 where the final concentration was 20 nM. Protein/DNA mixtures were loaded on NOVEX DNA retardation gels (Invitrogen) using 0.5× TBE buffer and run at 200-300V for 15-25 minutes. For complexes involving JUN proteins, the buffer was pre-cooled to 4 °C to prevent complex dissociation. Gels were dried and imaged using a phosphorimaging screen and a Typhoon 9400 imaging system.

Computational design of anti-MEQ

Anti-MEQ was designed using CLASSY with the HP/S/Ca energy function as previously reported (5). 46 human proteins and design homodimerization were used as negative design states.

Results

Four unique bZIPs are encoded by viral genomes

There are four bZIPs of viral origin described in the literature that are not closely related to any human bZIP. These are MEQ, HBZ, BZLF1, and K-bZIP. To compare these proteins to the human bZIPs, a phylogenetic tree was constructed using the leucine-zipper regions of the four viral proteins as well as 53 human bZIPs (Figure 1A). According to this analysis, all four viral bZIPs are quite diverged from human bZIPs. The sequences of the 4 viral bZIPs are aligned to several representative human sequences in Figure 1B. Human bZIPs have a highly conserved

basic region consisting of the motif (R/K)XX(R/K)N(R/K)XAAXX(S/C)RX(R/K)(R/K) (43), and a striking feature of the basic-region alignment is the presence of an invariant asparagine in almost all human bZIPs. The only two human families that do not have this asparagine are CREBZF (ZF, Zhangfei) and DDIT3 (CHOP), which are not known to bind DNA as homodimers but can bind as heterodimers (44, 45). An arginine, separated by 8 residues from the conserved asparagine, is strictly conserved in all human bZIPs. Both MEQ and BZLF1 conform well to this conserved motif and include the key asparagine and arginine residues. In contrast, the basic regions from HBZ and K-bZIP poorly match the basic-region motif, and neither contains the key conserved asparagine or arginine. The leucine-zipper regions of human bZIPs are 4-7 heptads long and are characterized by strong conservation of leucine every 7 amino acids. MEQ, HBZ, and to a lesser extent K-bZIP, have mostly canonical leucine-zipper regions. On the other hand, BZLF1 has a very short leucine zipper that is non-canonical, with only one coiled-coil **d**-position leucine (coiled-coil residues are traditionally labeled **a**-**f**, with **a** and **d** largely buried in the core, **e** and **g** on the periphery and **b**, **c** and **f** on the outside of the helical complex). BZLF1 has also been shown to be stabilized by an extended C-terminal region that makes contacts with the coiled coil (33). These observations are consistent with reports of both MEQ and BZLF1 binding DNA, whereas there is no direct evidence to support binding of DNA by HBZ (20, 33, 46). K-bZIP has been shown to directly bind DNA, though it is not clear whether the bZIP domain is involved (47).

Unlike HBZ, K-bZIP and BZLF1, which are found in viruses that infect humans, MEQ is encoded by an avian oncovirus. Because of the availability of a large number of human, but not avian, bZIP clones, we wanted to confirm that human bZIPs could be used as a reasonable substitute for chicken bZIPs. MEQ has been previously reported to interact with both human and mouse bZIP proteins (20). We also compared human bZIP sequences to chicken bZIP sequences and found them to be highly homologous (Figure S1). Considering just the coiled-coil interface positions that are most responsible for interactions (**adeg**), 85% of direct orthologues have greater than 90% identity. Additionally, all human bZIP families are conserved between human and chicken, except DDIT3, which is specific to humans.

Detection of viral-human bZIP interactions

Interactions between human and viral bZIPs were measured using a previously described protein microarray assay (5,6). The leucine-zipper regions of 33 representative human bZIPs were purified and printed onto aldehyde-derivatized glass slides along with leucine zippers from the 4 viral proteins (Table S1). All human bZIP families were represented on the arrays except for OASISb, which is very similar in its protein sequences and interaction profiles to OASIS. Each protein was then individually fluorescently labeled and used to probe the arrays at a concentration of ~160 nM, unless otherwise indicated. A total of 8 spots on the surface were used for each measurement. The fluorescence intensity of each spot was corrected for background, and the averages of the 8 values were converted into a score called S_{array}, a Z-score like measure, as described previously (Table S2) (5).

As in prior studies using this technique, there were several indications that the data are of good quality. First, interactions observed among human bZIPs (measured simultaneously with the viral-human interaction data) were highly consistent with previously published data (Figure S2)(6). Next, each heteromeric interaction was measured twice, once when the first protein was on the surface and again when it was in solution. Most interactions were observed in both directions. Further, interactions involving MEQ and HBZ were measured over a large range of concentrations and gave rise to similar interaction profiles (Figure 2B). Finally, many interactions observed between viral and human proteins were consistent with prior reports, as discussed below.

Most previously reported interactions involving the viral bZIPs were observed on the array and are indicated by green boxes in Figure 2A. Exceptions are boxed with green dotted lines in Figure 2A and include the interaction of HBZ with ATF4 and the interaction of MEQ with FOS. However, the HBZ—ATF4 interaction was reported to be weaker with just the leucine-zipper region (as was measured on the arrays) than in context of the entire protein (15). Also, the interaction of MEQ with FOS has been shown to be weak compared to other interactions of MEQ (17, 20). Several interactions previously reported to not occur were also not observed to interact on the arrays. These include HBZ self interaction, HBZ—FOS, BZLF1—FOS, and BZLF1—JUN (14, 48, 49). Both BZLF1 and K-bZIP have been reported to interact with CEBPA, but not as heterodimers (see Discussion).

Many previously unreported interactions were detected for HBZ. New partners included: MAF and MAFB, MAFG, ATF2 and ATF7, CEBPG (C/EBPγ), CREBZF, and ATF3. MEQ was observed to interact with known partners JUND and ATF7. New interactions identified included MEQ with NFIL3 (E4BP4) and BACH1. Interactions were also observed for MEQ with DDIT3 and NFE2, but these proteins are not conserved between human and chickens. DDIT3 is a member of the one human bZIP family that is not found in chickens. The NFE2 family is conserved in chickens but the human NFE2 protein does not have a direct ortholog, and the member of the family that does have a conserved ortholog, NFE2L1, is not observed to interact with MEQ.

BZLF1 was observed to self-associate strongly, but not to interact with any human bZIP peptides (Figure 2A). A BZLF1 construct with the C-terminal extension (BZLF1CT) also did not interact strongly with any human proteins. This construct gave greater fluorescence signal when probed against itself than against the version containing just the leucine zipper. BZFL1CT also showed strong signal at a lower concentration than BZLF1 with just the leucine zipper. This result is consistent with previous reports documenting stabilities in solution, and further demonstrates the ability of the arrays to accurately report relative affinities (Figure S3)(34, 50). K-bZIP interacted with itself stronger than with any other protein on the arrays. Weak interactions were observed with ATF2 and ATF7 when K-bZIP was in solution, but these interactions were not observed when K-bZIP was on the surface (Figure 2A).

A significant result of this experiment is that the leucine-zipper regions of MEQ and HBZ participate in multiple interactions with different human bZIPs, while BZLF1 and K-bZIP display almost exclusive homo-association (Figure 2A). Additionally, MEQ and HBZ each interact with a unique combination of partners (Figure 2C). HBZ interacts with many of the same proteins as ATF3 and FOS, but is distinguished by many other strong interactions that are not made by these proteins, including interactions with both the small and large MAF families, CEBPG, and CREBZF. MEQ also has a similar profile to human ATF3 and FOS, but additionally interacts strongly with NFIL3.

Validation of novel interactions of HBZ and MEQ in solution

To validate novel interactions detected on the protein microarrays we tested associations using circular dichroism (CD). Proteins consisting of the bZIP domain (basic region plus leucine zipper) were used for these experiments (see Methods, Table S1). For NFIL3, the chicken and human proteins are identical in this region. For the MAF proteins, the extended homology region that contains an auxiliary DNA binding domain was included (51). We first tested JUN for interaction with HBZ and MEQ. JUN has been reported to interact with both MEQ and HBZ and was also observed to interact with both on the arrays. HBZ and Jun each at 40 μM were mixed together and the CD spectrum was measured (Figure 3A). Spectra were also recorded for each protein in isolation. The spectra of each individual protein, as well as the mixture, had minima at 208 and 222 nm, which is characteristic of coiled coils. The observed mean residue ellipticity at 222 nm ($[\theta]_{222}$) is consistent with the expected helical content for

these peptides forming coiled coils, as the leucine zipper accounts for ~50% of the sequence (52). The mixture also had increased signal compared to the sum of the individual proteins, indicating a hetero-association. Similar results were observed for MEQ and JUN (Figure 3B).

We next tested HBZ against the newly identified partners ATF2, CEBPG, CREBZF, MAFG, and MAFB. Thermal melts monitored by CD were performed with each protein at a concentration of 4 μM and the mixture at 8 μM. Thermal melts were also carried out for HBZ with JUN (Figure 3, C-H). Over a large range in temperature, all mixtures had increased signal over the sum of the spectra for the individual proteins, confirming the interactions. We then performed thermal melts of MEQ with NFIL3 and with JUN (Figure 3I, J). Again the mixture had increased signal over that expected for non-interacting proteins. Two pairs not observed to interact on the arrays, HBZ with NFIL3 and MEQ with MAFB, also were not observed to interact in solution (Figure 3K, L). Thus, all protein pairs tested in solution agreed well with the results of the protein array assay.

Characterization of HBZ interactions with human proteins in the presence of DNA

We tested whether HBZ could prevent its human bZIP interaction partners from binding DNA and/or whether heteromeric HBZ complexes could themselves bind DNA. MAFB and MAFG were tested in a gel-shift assay using a MARE site (40). Both bound MARE DNA as homodimers at a concentration of 4 nM, but HBZ did not bind even at a 100-fold higher concentration. Surprisingly, when highly purified HBZ at increasing concentrations was mixed with a constant concentration of either highly purified MAFB or MAFG, an additional shifted band of greater mobility appeared (Figure 4A). We inferred that this band included both HBZ and MAFB or MAFG. To determine whether formation of this complex was dependant on the basic region of HBZ, a leucine-zipper-only version of HBZ, HBZLZ, was mixed with the MAF proteins. The amount of MAF protein bound to DNA was decreased, though a higher concentration of HBZLZ was required. No additional complex was detected (Figure 4B). This is the first evidence, to our knowledge, that HBZ can directly bind to DNA, and that this binding depends on the basic region. The stoichiometry and structure of the observed heterocomplex remain unknown. We also tested whether ATF2 or CEBPG could bind DNA in complex with HBZ. Both ATF2 and CEBPG at 20 nM were prevented from binding MARE DNA by HBZ, but no additional band was formed (Figure 4C). CREBZF was not tested in complex with HBZ on DNA as CREBZF is not known to bind DNA by itself (44).

MAFG also binds to the AP-1 site and was tested for binding in combination with HBZ. In contrast to the MARE site, HBZ decreased the binding of MAFG to the AP-1 site without formation of any additional shifted bands (Figure 4D). Both the AP-1 and the MARE sites contain the core consensus binding site TGA(C/G)TCA. The MAF proteins have an auxiliary binding domain that is responsible for binding flanking residues of the MARE site (51). At the middle of the binding site, position 0, the MARE site we used has a C and the AP-1 site contains a G. To determine if this middle position can affect DNA binding by HBZ:MAFG complexes, the 0 position in MARE was changed to a G and the same position in AP-1 was changed to a C. The mutant sites had similar binding properties to unchanged sites, suggesting that the middle position is not the key element that influences HBZ—MAFG heteroassociation on AP-1 vs. MARE (Figure 4E, F). This suggests that bases flanking the core site are important for HBZ binding.

Characterization of MEQ and NFIL3 binding to DNA

To determine whether NFIL3 and MEQ could bind DNA as heterodimers we tested several known bZIP-binding sites. AP-1, also known as TRE, is a site bound by JUN and by FOS-JUN heterodimer (53). CAAT contains the consensus site for the CEBP family of bZIPs (54). CRE1 and CRE2 are two CRE-like sites that have been previously used in DNA binding studies with

MEQ and NFIL3 and are each one change away from the consensus CRE site TGACGTCA (20,42). Also tested was the MDVORI site, which is derived from the origin of replication of Marek's disease virus. MEQ has previously been shown to bind this site as a homodimer (20). In a gel-shift assay neither MEQ nor NFIL3 bound strongly to the negative control sites TFIID or NF-κB at 80 nM. Only MEQ bound strongly to the AP-1 site and only NFIL3 bound strongly to the CAAT site. Both MEQ and NFIL3 bound the CRE1 and CRE2 sites, though NFIL3 bound more strongly. For both of these sites there appeared to be some heterodimer formation, but the predominant species was the NFIL3 homodimer. Interestingly, NFIL3 bound to the MDVORI site, but weaker than MEQ did. The mixture on the MDVORI site was composed of primarily MEQ homodimers (Figure 5A).

We also wanted to know if MEQ and NFIL3 could bind a DNA site predominantly as a heterodimer. Previously it has been shown that heterodimer sites can be constructed by taking consensus half-sites for each of two interacting bZIPs (55). A DNA site was constructed that contains the consensus half-sites for MEQ (ACAC) and NFIL3 (GTAA), referred to in Figure 5C and below as MEQ/NFIL3 (20,56). This site has only two changes from the MDVORI site, at positions +1 and +3. This hybrid site was bound as a homodimer by both MEQ and NFIL3. NFIL3 bound tighter than MEQ, and when both proteins were mixed, the predominant species bound to the site was the heterocomplex, with mobility between the two homodimers (Figure 5A).

The MDVORI probe used in Figure 5 was 30 base pairs long, and to further probe the nature of a MEQ—NFIL3 interaction we tested whether NFIL3 bound at a similar location as MEQ. Competition gel-shift experiments were performed to test this. MEQ and NFIL3 were individually incubated with radiolabeled MDVORI site and with cold competitor DNA encoding either the MDVORI site or a variant of it. Single-base substitutions were made at 10 consecutive positions in the site. Additionally, 2 double substitutions and a triple-mutant site were constructed. Changes that affected MEQ binding by at least 2-fold were localized toward the 5′ half of the MDVORI site (Figure 5B). Substitutions that weakened MEQ binding included -4C, - 3A, and -1A. The change of -2T strengthened MEQ binding. The double mutant of -3A:-1A decreased binding more than either individual substitution. NFIL3 binding was decreased by the changes -1A, +1C, +2G, and +4C. The substitutions -3A and +3A increased binding of NFIL3. Combining -2T and +1C decreased binding further. The changes of -1A and +2G decreased binding individually, but when both were together in combination with -3A, the triple mutant had no decrease in binding (Figure 5B). These 13 altered sites were also tested for direct binding to MEQ and NFIL3 and the results were consistent with the competition binding experiments (Figure S4). Additionally, significant heterodimer formation by MEQ and NFIL3 was observed on the +3A site, consistent with results using the hybrid site in Figure 5A (Figure S4). Several things are apparent from this experiment. First, mutations on the 5′ side of the site affect binding to MEQ, while those toward the 3′ end, and at the last two positions of the left half-site, affect binding to NFIL3. Second, most DNA base changes have differential effects on the binding of MEQ and NFIL3, demonstrating they indeed have different binding specificities. Third, MEQ and NFIL3 bind at a similar location on the MDVORI DNA site.

Generation of a specific inhibitor of MEQ dimerization

Specific inhibitors of bZIP interactions could provide valuable tools for elucidating function and could potentially serve to validate transcription factors as therapeutic targets. To generate a specific peptide to bind MEQ, that could potentially act as a dominant-negative inhibitor, we used a recently published computational design method called CLASSY (5). CLASSY was used to automatically design a peptide sequence predicted to bind MEQ but to have minimal binding to any human bZIP or to itself. The designed 42-residue anti-MEQ peptide was tested

for its ability to bind MEQ using bZIP protein arrays including anti-MEQ, MEQ, and a panel of 32 human bZIPs (these included all the human peptides tested previously except DDIT3, which is specific to humans). Anti-MEQ bound MEQ stronger than any human protein (Figure 6A). The other proteins that anti-MEQ bound strongest are the ATF2 family proteins ATF2 and ATF7, followed by JUN and BATF3. Even at the highest concentration tested, 2000 nM, anti-MEQ bound MEQ and the ATF2 family proteins preferentially to other bZIPs. Anti-MEQ was not observed to interact with itself on the arrays. These results demonstrate that anti-MEQ is specific for binding to MEQ.

To compare the stability of the anti-MEQ—MEQ complex with that of other MEQ interactions, we probed MEQ against an array including MEQ, anti-MEQ, and the panel of 32 human peptides. MEQ interacted with anti-MEQ as strongly as it interacted with JUN, which was MEQ's strongest human interaction partner observed on the array (Figure 6A). The three strongest off-target interactions, ATF2, JUN, and BATF3, were also tested as solution probes. ATF2 bound anti-MEQ strongly compared to its strongest interactions on the array. In contrast, JUN and BATF had much weaker interactions with anti-MEQ. Overall these results suggest that anti-MEQ has high affinity for, and is specific for, interaction with MEQ.

The interaction of MEQ and anti-MEQ in solution was studied using a tag-less version of anti-MEQ (see Methods). CD spectra showed that anti-MEQ is mostly unfolded at 40 μM, and when combined with 40 μM MEQ the mixture has more signal than either MEQ or anti-MEQ alone, indicating an interaction. The mixture also has a spectrum characteristic of a coiled coil (Figure 6B). Thermal melts of anti-MEQ mixed with either MEQ and ATF2 were performed at 4 μM of each protein and 8 μM total protein for the mixture (Figure 6C, D). The temperature of half denaturation (T_m) for anti-MEQ was 12.8 °C, for MEQ was 35.2 °C, and for ATF2 was 36.7 °C. The T_m for anti-MEQ in complex with MEQ was 40.5 °C, and thus the hetero-association is more stable than either the homo-association of MEQ or anti-MEQ. The T_m of ATF2 in complex with MEQ was 31.8 °C. JUN, a strong interaction partner for MEQ, has a T_m in complex with MEQ of 41.3 °C. These results are consistent with the array data. A helical wheel diagram depicting the predicted interaction geometry of MEQ and anti-MEQ is shown in Figure 6E. The design has leucine residues at 5 consecutive **d**-positions, imparting stability to the complex (57). It also introduces a complementary asparagine residue to interact with an asparagine at an **a**-position in MEQ; this interaction is known to favor parallel dimer formation (58). The **e**- and **g**-positions of anti-MEQ are complementary to those in MEQ, and two rather uncommon cysteine residues at **a** positions are predicted to lie across from designed alanine and lysine residues. Lysine at core **a** positions also favors dimer formation (59). Two lysines at **a** positions are complementary to glutamate residues at **g** position on the opposite helix. These **a**-**g**′ interactions have previously been shown to make important contributions to specificity (5, 38).

To test whether anti-MEQ could prevent MEQ from binding DNA, 20 nM MEQ was incubated with increasing amounts of anti-MEQ and then radiolabeled MDVORI DNA was added to the reactions. Anti-MEQ prevented MEQ binding of DNA, with an IC_{50} of less than 500 nM (Figure 7A). Binding of MEQ to AP-1 DNA was also inhibited by anti-MEQ (data not shown). The experiment was repeated with 20 nM JUN and the AP-1 DNA site. No decrease in JUN binding was observed even at 12.5 μM anti-MEQ (Figure 7B). The strongest off-target interaction for anti-MEQ, ATF2, was also tested. At 20 nM ATF2 no decrease in binding was observed when incubated with anti-MEQ (Figure 7C). At 4 nM ATF2, anti-MEQ decreased ATF2 binding, but at higher concentrations than required for preventing MEQ binding (Figure 7D). These results show that anti-MEQ can prevent MEQ from binding DNA at a lower concentration than it inhibits its strongest off-target interaction.

Discussion

The bZIP transcription factors function by forming homodimers or heterodimers with other bZIP proteins. In this context, viruses use bZIP proteins in a number of distinct ways that are illuminated by the systematic study we present here. Several viral bZIPs that have high sequence identity to host homologues maintain the interaction patterns of the host bZIPs. Examples include v-FOS, v-JUN, and v-MAF (7-9). The viral bZIPs HBZ and MEQ are not closely related to any other bZIPs, and they have distinct interaction profiles compared to the human bZIPs. K-bZIP and BZLF1 are also not highly conserved, but the bZIP domains of these two viral proteins primarily self-associate.

For MEQ and HBZ, we have uncovered new interactions that suggest possible mechanisms of action of these proteins. The mechanism of HBZ protein function has been somewhat of a mystery. The non-canonical basic region of this protein argues against direct DNA binding, yet HBZ was shown previously to have a strong activation domain, suggesting that it might function to regulate transcription when complexed with human bZIP proteins and DNA (15, 60). Additionally, HBZ has been shown to stimulate the transcriptional activity of JUND(13). However, data so far have not supported a direct interaction of HBZ itself with DNA. Here we present the first evidence that HBZ can directly bind DNA. HBZ can bind a MARE DNA site with MAFB or MAFG. This binding of DNA is specific and is dependent both on the HBZ basic region and on DNA that flanks the central binding site. While most bZIPs bind a 4-5 base pair half site, different flanking regions around an AP-1 site have previously been shown to have different affinities for binding to JUN/FOS heterodimers (61). The HBZ ternary complex that we observed on DNA with either MAFB or MAFG was weaker than MAF—DNA complexes. Also the HBZ—MAF complexes occurred at higher concentrations of HBZ relative to MAF protein. Because the sequence of the HBZ basic region is unique, it may have a distinct DNA-binding specificity, and it remains a possibility that higher affinity sites for HBZ in association with MAF proteins exist.

The MAF proteins belong to two classes: the four large MAF proteins, which contain a transcriptional activation domain, and the three small MAF proteins that don't. The small MAFs interact with the NFE2 and BACH families of bZIPs and play a major role in the response to oxidative stress (62). The large MAF proteins are similar to the JUN proteins in that both are involved in cell growth and proliferation, both are proto-oncogenes and can cause cellular transformation, and both have retroviral homologues (63,64). They also have been reported to share similar downstream targets in inducing cellular transformation (65).

Other proteins we confirmed to interact with HBZ *in vitro* are CEBPG, ATF2, and CREBZF. The CEBP family of bZIPs is involved in cell growth and differentiation. CEBPG forms heterodimers with CEBP family proteins to repress their transcriptional activity (66). ATF2 has been shown to stimulate JUN-mediated cellular transformation (67). CREBZF was identified as having a role in herpes simplex virus gene expression (68). CREBZF also interacts with ATF4, a known partner of HBZ (15,44). With ATF2 and CEBPG, it remains to be seen whether HBZ heterodimers can bind DNA sites, or if HBZ functions primarily by preventing binding of these partners to target sites. Neither HBZ nor CREBZF have been shown to bind DNA as homodimers, suggesting that they have intrinsically weaker affinities for DNA and together would not be likely to bind DNA as a heterodimer. These newly reported partners, along with other known partners, suggest that HBZ has the potential to impact several different transcriptional pathways.

It was recently shown that MEQ homodimers alone are not sufficient to induce transformation, suggesting that heterodimer formation with other bZIPs is necessary (17). JUN has been shown to be an important MEQ partner, required for cellular transformation mediated by MEQ, but

it is likely that other interaction partners are also functionally important. Here we identified a previously unreported bZIP partner, NFIL3, and showed that it can form heterodimers with MEQ on DNA. NFIL3 was first identified as a transcriptional repressor that bound the adenovirus E4 promoter, and was later shown to have an activating role associated with anti-apoptotic activity. NFIL3 is also involved in regulating circadian rhythms (56,69,70). NFIL3 was further shown in the hepatitis B virus to both repress viral gene expression as well as viral replication (71). In this context, it is interesting that NFIL3 can bind to the MDVORI site as a homodimer. The MDVORI site from the origin of replication of MDV is also situated between a bidirectional promoter that MEQ has been shown to repress as a homodimer (20,21). There may exist functionally significant sites that MEQ and NFIL3 can bind as a heterodimer with greater affinity than either homodimer. It will be important to determine what role NFIL3 has on the MDV life cycle, both alone and in combination with MEQ.

Other novel interactions with bZIP families detected on the arrays but not tested further are HBZ with ATF3, and MEQ with BACH1. Based on the intensity of the fluorescence signal, these interactions are likely to be weaker than the other interactions tested, but they may be significant. Also, numerous interactions that we did not assay are highly likely to occur involving paralogs of the proteins tested here. Although these interactions need to be confirmed experimentally, most bZIP paralogs are highly similar to each other and have been shown to share similar interaction profiles (5,6,39).

An interesting result is that the leucine-zipper regions of BZLF1 and K-bZIP preferentially self-associate. Both proteins are reported to interact with CEBPA, but this pairing was not observed in our array experiments. Basic residues were required for this interaction in the case of BZLF1, and both proteins were observed to interact with CEBPA as higher-order multimers and not as heterodimers (31,32). Our observation that the leucine zippers are not sufficient for these interactions is consistent with those studies. It is not surprising, given the unique structure of BZLF1, that it does not form canonical interactions with human BZIPs.

MDV is the first oncogenic virus for which a vaccine was made available to control the disease, but increasing viral resistance is becoming a real concern to the poultry industry. Further, MDV has proven valuable as a model oncogenic virus, and deletion and knockdown experiments have demonstrated the necessity of MEQ for oncogenic transformation (18). It has also been reported that a virus encoding a MEQ protein that cannot form homodimers or heterodimers has a complete loss of oncogenicity, suggesting that the function of MEQ could be inhibited by preventing MEQ from interacting with bZIPs (19). We showed that a computationally designed anti-MEQ peptide can prevent MEQ from binding DNA in a specific manner, indicating that anti-MEQ could be a useful reagent for studying the role of MEQ on the oncogenic properties of MDV. If necessary to achieve higher affinity, the anti-MEQ peptide could potentially be further stabilized through the addition of an acidic peptide extension that interacts with the basic region, as has been demonstrated for numerous other coiled coils by the Vinson laboratory (41).

In summary, we have shown that coiled-coil arrays are a powerful method for broadly surveying the interaction properties of viral bZIP dimerization domains. Comprehensive testing for *in vitro* interactions with all human bZIP families is an important step in exploring the functions of these proteins. Further, we have validated that several newly discovered viral-host complexes can bind to DNA, suggesting a mechanism by which viruses hijack cellular transcriptional control. Determining which of the bZIPs that can associate *in vitro* also interact with functional consequences *in vivo* will be an important next step.

Supplementary Material

Refer to Web version on PubMed Central for supplementary material.

Acknowledgments

We thank the MIT BioMicro center for arraying instrumentation, J. Fisher for technical assistance in cloning and protein purification and the Laub lab for use of space and equipment. We thank members of the Keating laboratory for comments on the manuscript.

This work was supported by NIH award GM067681 and used computer equipment purchased under NSF award 0216437.

References

1. Hardwick JM, Bellows DS. Viral versus cellular BCL-2 proteins. Cell Death Differ 2003;10:S68–76. [PubMed: 12655348]
2. Kvansakul M, Yang H, Fairlie WD, Czabotar PE, Fischer SF, Perugini MA, Huang DC, Colman PM. Vaccinia virus anti-apoptotic F1L is a novel Bcl-2-like domain-swapped dimer that binds a highly selective subset of BH3-containing death ligands. Cell Death Differ 2008;15:1564–1571. [PubMed: 18551131]
3. Daury L, Busson M, Tourkine N, Casas F, Cassar-Malek I, Wrutniak-Cabello C, Castellazzi M, Cabello G. Opposing functions of ATF2 and Fos-like transcription factors in c-Jun-mediated myogenin expression and terminal differentiation of avian myoblasts. Oncogene 2001;20:7998–8008. [PubMed: 11753683]
4. Hai T, Curran T. Cross-family dimerization of transcription factors Fos/Jun and ATF/CREB alters DNA binding specificity. Proc Natl Acad Sci U S A 1991;88:3720–3724. [PubMed: 1827203]
5. Grigoryan G, Reinke AW, Keating AE. Design of protein-interaction specificity gives selective bZIP-binding peptides. Nature 2009;458:859–864. [PubMed: 19370028]
6. Newman JRS, Keating AE. Comprehensive Identification of Human bZIP Interactions with Coiled-Coil Arrays. Science 2003;300:2097–2101. [PubMed: 12805554]
7. van Straaten F, Muller R, Curran T, Van Beveren C, Verma IM. Complete nucleotide sequence of a human c-onc gene: deduced amino acid sequence of the human c-fos protein. Proc Natl Acad Sci U S A 1983;80:3183–3187. [PubMed: 6574479]
8. Bos TJ, Rauscher FJ 3rd, Curran T, Vogt PK. The carboxy terminus of the viral Jun oncoprotein is required for complex formation with the cellular Fos protein. Oncogene 1989;4:123–126. [PubMed: 2494630]
9. Kataoka K, Nishizawa M, Kawai S. Structure-function analysis of the maf oncogene product, a member of the b-Zip protein family. J Virol 1993;67:2133–2141. [PubMed: 8383235]
10. Mesnard JM, Barbeau B, Devaux C. HBZ, a new important player in the mystery of Adult-T- cell leukemia. Blood 2006;108:3979–3982. [PubMed: 16917009]
11. Satou Y, Yasunaga Ji, Yoshida M, Matsuoka M. HTLV-I basic leucine zipper factor gene mRNA supports proliferation of adult T cell leukemia cells. Proc Natl Acad Sci U S A 2006;103:720–725. [PubMed: 16407133]
12. Lemasson I, Lewis MR, Polakowski N, Hivin P, Cavanagh MH, Thebault S, Barbeau B, Nyborg JK, Mesnard JM. Human T-Cell Leukemia Virus Type 1 (HTLV-1) bZIP Protein Interacts with the Cellular Transcription Factor CREB To Inhibit HTLV-1 Transcription. J Virol 2007;81:1543–1553. [PubMed: 17151132]
13. Thebault S, Basbous J, Hivin P, Devaux C, Mesnard JM. HBZ interacts with JunD and stimulates its transcriptional activity. FEBS Lett 2004;562:165–170. [PubMed: 15044019]
14. Basbous J, Arpin C, Gaudray G, Piechaczyk M, Devaux C, Mesnard JM. The HBZ Factor of Human T-cell Leukemia Virus Type I Dimerizes with Transcription Factors JunB and c-Jun and Modulates Their Transcriptional Activity. J Biol Chem 2003;278:43620–43627. [PubMed: 12937177]
15. Gaudray G, Gachon F, Basbous J, Biard-Piechaczyk M, Devaux C, Mesnard JM. The Complementary Strand of the Human T-Cell Leukemia Virus Type 1 RNA Genome Encodes a bZIP Transcription

Factor That Down-Regulates Viral Transcription. J Virol 2002;76:12813–12822. [PubMed: 12438606]

16. Nair V. Evolution of Marek's disease - A paradigm for incessant race between the pathogen and the host. Vet J 2005;170:175–183. [PubMed: 16129338]
17. Suchodolski PF, Izumiya Y, Lupiani B, Ajithdoss DK, Gilad O, Lee LF, Kung HJ, Reddy SM. Homodimerization of Marek's Disease Virus-Encoded Meq Protein Is Not Sufficient for Transformation of Lymphocytes in Chickens. J Virol 2009;83:859–869. [PubMed: 18971275]
18. Levy AM, Gilad O, Xia L, Izumiya Y, Choi J, Tsalenko A, Yakhini Z, Witter R, Lee L, Cardona CJ, Kung HJ. Marek's disease virus Meq transforms chicken cells via the v-Jun transcriptional cascade: A converging transforming pathway for avian oncoviruses. Proc Natl Acad Sci U S A 2005;102:14831–14836. [PubMed: 16203997]
19. Brown AC, Smith LP, Kgosana L, Baigent SJ, Nair V, Allday MJ. Homodimerization of the Meq Viral Oncoprotein Is Necessary for Induction of T-Cell Lymphoma by Marek's Disease Virus. J Virol 2009;83:11142–11151. [PubMed: 19692466]
20. Levy AM, Izumiya Y, Brunovskis P, Xia L, Parcells MS, Reddy SM, Lee L, Chen HW, Kung HJ. Characterization of the Chromosomal Binding Sites and Dimerization Partners of the Viral Oncoprotein Meq in Marek's Disease Virus-Transformed T Cells. J Virol 2003;77:12841–12851. [PubMed: 14610205]
21. Qian Z, Brunovskis P, Lee L, Vogt PK, Kung HJ. Novel DNA binding specificities of a putative herpesvirus bZIP oncoprotein. J Virol 1996;70:7161–7170. [PubMed: 8794363]
22. Qian Z, Brunovskis P, Rauscher F 3rd, Lee L, Kung HJ. Transactivation activity of Meq, a Marek's disease herpesvirus bZIP protein persistently expressed in latently infected transformed T cells. J Virol 1995;69:4037–4044. [PubMed: 7769661]
23. Thomas FS. The pleiotropic effects of Kaposi's sarcoma herpesvirus. J Pathol 2006;208:187–198. [PubMed: 16362980]
24. Kutok JL, Wang F. SPECTRUM OF EPSTEIN-BARR VIRUSâ€“ASSOCIATED DISEASES. Annu Rev Pathol-mech 2006;1:375–404.
25. Lin SF, Robinson DR, Miller G, Kung HJ. Kaposi's Sarcoma-Associated Herpesvirus Encodes a bZIP Protein with Homology to BZLF1 of Epstein-Barr Virus. J Virol 1999;73:1909–1917. [PubMed: 9971770]
26. Countryman J, Jenson H, Seibl R, Wolf H, Miller G. Polymorphic proteins encoded within BZLF1 of defective and standard Epstein-Barr viruses disrupt latency. J Virol 1987;61:3672–3679. [PubMed: 2824806]
27. Schepers A, Pich D, Hammerschmidt W. Activation oforiLyt,the Lytic Origin of DNA Replication of Epstein-Barr Virus, by BZLF1. Virology 1996;220:367–376. [PubMed: 8661388]
28. Rossetto C, Yamboliev I, Pari GS. Kaposi's Sarcoma-Associated Herpesvirus/Human Herpesvirus 8 K-bZIP modulates LANA mediated suppression of lytic origin-dependent DNA synthesis. J Virol 2009:JVI.00922–00909.
29. Ellison TJ, Izumiya Y, Izumiya C, Luciw PA, Kung HJ. A comprehensive analysis of recruitment and transactivation potential of K-Rta and K-bZIP during reactivation of Kaposi's sarcoma-associated herpesvirus. Virology 2009;387:76–88. [PubMed: 19269659]
30. Sinclair AJ. bZIP proteins of human gammaherpesviruses. J Gen Virol 2003;84:1941–1949. [PubMed: 12867624]
31. Wu FY, Wang SE, Chen H, Wang L, Hayward SD, Hayward GS. CCAAT/Enhancer Binding Protein {alpha} Binds to the Epstein-Barr Virus (EBV) ZTA Protein through Oligomeric Interactions and Contributes to Cooperative Transcriptional Activation of the ZTA Promoter through Direct Binding to the ZII and ZIIIB Motifs during Induction of the EBV Lytic Cycle. J Virol 2004;78:4847–4865. [PubMed: 15078966]
32. Wu FY, Wang SE, Tang QQ, Fujimuro M, Chiou CJ, Zheng Q, Chen H, Hayward SD, Lane MD, Hayward GS. Cell Cycle Arrest by Kaposi's Sarcoma-Associated Herpesvirus Replication-Associated Protein Is Mediated at both the Transcriptional and Posttranslational Levels by Binding to CCAAT/Enhancer-Binding Protein {alpha} and p21CIP-1. J Virol 2003;77:8893–8914. [PubMed: 12885907]

33. Petosa C, Morand P, Baudin F, Moulin M, Artero JB, Muller CW. Structural Basis of Lytic Cycle Activation by the Epstein-Barr Virus ZEBRA Protein. Mol Cell 2006;21:565–572. [PubMed: 16483937]
34. Hicks MR, Al-Mehairi SS, Sinclair AJ. The Zipper Region of Epstein-Barr Virus bZIP Transcription Factor Zta Is Necessary but Not Sufficient To Direct DNA Binding. J Virol 2003;77:8173–8177. [PubMed: 12829857]
35. Hoover DM, Lubkowski J. DNAWorks: an automated method for designing oligonucleotides for PCR-based gene synthesis. Nucleic Acids Res 2002;30:e43. [PubMed: 12000848]
36. Gerhard DS, Wagner L, Feingold EA, Shenmen CM, Grouse LH, Schuler G, Klein SL, Old S, Rasooly R, Good P, Guyer M, Peck AM, Derge JG, Lipman D, Collins FS, Jang W, Sherry S, Feolo M, Misquitta L, Lee E, Rotmistrovsky K, Greenhut SF, Schaefer CF, Buetow K, Bonner TI, Haussler D, Kent J, Kiekhaus M, Furey T, Brent M, Prange C, Schreiber K, Shapiro N, Bhat NK, Hopkins RF, Hsie F, Driscoll T, Soares MB, Casavant TL, Scheetz TE, Brown-stein MJ, Usdin TB, Toshiyuki S, Carninci P, Piao Y, Dudekula DB, Ko MS, Kawakami K, Suzuki Y, Sugano S, Gruber CE, Smith MR, Simmons B, Moore T, Waterman R, Johnson SL, Ruan Y, Wei CL, Mathavan S, Gunaratne PH, Wu J, Garcia AM, Hulyk SW, Fuh E, Yuan Y, Sneed A, Kowis C, Hodgson A, Muzny DM, McPherson J, Gibbs RA, Fahey J, Helton E, Ketteman M, Madan A, Rodrigues S, Sanchez A, Whiting M, Madari A, Young AC, Wetherby KD, Granite SJ, Kwong PN, Brinkley CP, Pearson RL, Bouffard GG, Blakesly RW, Green ED, Dickson MC, Rodriguez AC, Grimwood J, Schmutz J, Myers RM, Butterfield YS, Griffith M, Griffith OL, Krzywinski MI, Liao N, Morin R, Palmquist D, et al. The status, quality, and expansion of the NIH full-length cDNA project: the Mammalian Gene Collection (MGC). Genome Res 2004;14:2121–2127. [PubMed: 15489334]
37. Witt AE, Hines LM, Collins NL, Hu Y, Gunawardane RN, Moreira D, Raphael J, Jepson D, Koundinya M, Rolfs A, Taron B, Isakoff SJ, Brugge JS, LaBaer J. Functional proteomics approach to investigate the biological activities of cDNAs implicated in breast cancer. J Proteome Res 2006;5:599–610. [PubMed: 16512675]
38. Reinke AW, Grant RA, Keating AE. A synthetic coiled-coil interactome provides heterospecific modules for molecular engineering. Submitted.
39. Amoutzias GD, Veron AS, Weiner J 3rd, Robinson-Rechavi M, Bornberg-Bauer E, Oliver SG, Robertson DL. One billion years of bZIP transcription factor evolution: conservation and change in dimerization and DNA-binding site specificity. Mol Biol Evol 2007;24:827–835. [PubMed: 17194801]
40. Kataoka K, Fujiwara KT, Noda M, Nishizawa M. MafB, a new Maf family transcription activator that can associate with Maf and Fos but not with Jun. Mol Cell Biol 1994;14:7581–7591. [PubMed: 7935473]
41. Acharya A, Rishi V, Moll J, Vinson C. Experimental identification of homodimerizing B-ZIP families in Homo sapiens. J Struct Biol 2006;155:130–139. [PubMed: 16725346]
42. Chen WJ, Lewis KS, Chandra G, Cogswell JP, Stinnett SW, Kadwell SH, Gray JG. Characterization of human E4BP4, a phosphorylated bZIP factor. BBA-gene Struct Expr 1995;1264:388–396.
43. Adya N, Zhao LJ, Huang W, Boros I, Giam CZ. Expansion of CREB's DNA recognition specificity by Tax results from interaction with Ala-Ala-Arg at positions 282-284 near the conserved DNA-binding domain of CREB. Proc Natl Acad Sci U S A 1994;91:5642–5646. [PubMed: 8202541]
44. Hogan MR, Cockram GP, Lu R. Cooperative interaction of Zhangfei and ATF4 in transactivation of the cyclic AMP response element. FEBS Lett 2006;580:58–62. [PubMed: 16343488]
45. Ubeda M, Wang XZ, Zinszner H, Wu I, Habener JF, Ron D. Stress-induced binding of the transcriptional factor CHOP to a novel DNA control element. Mol Cell Biol 1996;16:1479–1489. [PubMed: 8657121]
46. Hivin P, Arpin-Andre C, Clerc I, Barbeau B, Mesnard JM. A modified version of a Fos-associated cluster in HBZ affects Jun transcriptional potency. Nucl Acids Res 2006;34:2761–2772. [PubMed: 16717281]
47. Lefort S, Soucy-Faulkner A, Grandvaux N, Flamand L. Binding of Kaposi's Sarcoma-Associated Herpesvirus K-bZIP to Interferon-Responsive Factor 3 Elements Modulates Antiviral Gene Expression. J Virol 2007;81:10950–10960. [PubMed: 17652396]

48. Chang YN, Dong DL, Hayward GS, Hayward SD. The Epstein-Barr virus Zta transactivator: a member of the bZIP family with unique DNA-binding specificity and a dimerization domain that lacks the characteristic heptad leucine zipper motif. J Virol 1990;64:3358–3369. [PubMed: 2161945]
49. Matsumoto J, Ohshima T, Isono O, Shimotohno K. HTLV-1 HBZ suppresses AP-1 activity by impairing both the DNA-binding ability and the stability of c-Jun protein. Oncogene 2005;24:1001–1010. [PubMed: 15592508]
50. Hicks MR, Balesaria S, Medina-Palazon C, Pandya MJ, Woolfson DN, Sinclair AJ. Biophysical analysis of natural variants of the multimerization region of Epstein-Barr virus lytic-switch protein BZLF1. J Virol 2001;75:5381–5384. [PubMed: 11333921]
51. Kerppola TK, Curran T. A conserved region adjacent to the basic domain is required for recognition of an extended DNA binding site by Maf/Nrl family proteins. Oncogene 1994;9:3149–3158. [PubMed: 7936637]
52. Chen YH, Yang JT, Chau KH. Determination of the helix and beta form of proteins in aqueous solution by circular dichroism. Biochemistry 1974;13:3350–3359. [PubMed: 4366945]
53. Rauscher FJ Iii, Sambucetti LC, Curran T, Distel RJ, Spiegelman BM. Common DNA binding site for Fos protein complexesand transcription factor AP-1. Cell 1988;52:471–480. [PubMed: 3125983]
54. Oikarinen J, Hatamochi A, de Crombrugghe B. Separate binding sites for nuclear factor 1 and a CCAAT DNA binding factor in the mouse alpha 2(I) collagen promoter. J Biol Chem 1987;262:11064–11070. [PubMed: 3038906]
55. Vinson CR, Hai T, Boyd SM. Dimerization specificity of the leucine zipper-containing bZIP motif on DNA binding: prediction and rational design. Genes Dev 1993;7:1047–1058. [PubMed: 8504929]
56. Cowell IG, Skinner A, Hurst HC. Transcriptional repression by a novel member of the bZIP family of transcription factors. Mol Cell Biol 1992;12:3070–3077. [PubMed: 1620116]
57. Moitra J, Szilak L, Krylov D, Vinson C. Leucine is the most stabilizing aliphatic amino acid in the d position of a dimeric leucine zipper coiled coil. Biochemistry 1997;36:12567–12573. [PubMed: 9376362]
58. Harbury PB, Zhang T, Kim PS, Alber T. A switch between two-, three-, and four-stranded coiled coils in GCN4 leucine zipper mutants. Science 1993;262:1401–1407. [PubMed: 8248779]
59. Campbell KM, Sholders AJ, Lumb KJ. Contribution of Buried Lysine Residues to the Oligomerization Specificity and Stability of the Fos Coiled Coil. Biochemistry 2002;41:4866–4871. [PubMed: 11939781]
60. Kuhlmann AS, Villaudy J, Gazzolo L, Castellazzi M, Mesnard JM, Duc Dodon M. HTLV-1 HBZ cooperates with JunD to enhance transcription of the human telomerase reverse transcriptase gene (hTERT). Retrovirology 2007;4:92. [PubMed: 18078517]
61. Ryseck RP, Bravo R. c-JUN, JUN B, and JUN D differ in their binding affinities to AP-1 and CRE consensus sequences: effect of FOS proteins. Oncogene 1991;6:533–542. [PubMed: 1827665]
62. Katsuoka F, Motohashi H, Ishii T, Aburatani H, Engel JD, Yamamoto M. Genetic evidence that small maf proteins are essential for the activation of antioxidant response element-dependent genes. Mol Cell Biol 2005;25:8044–8051. [PubMed: 16135796]
63. Vogt PK. Jun, the oncoprotein. Oncogene 2001;20:2365–2377. [PubMed: 11402333]
64. Pouponnot C, Sii-Felice K, Hmitou I, Rocques N, Lecoin L, Druillennec S, Felder-Schmittbuhl MP, Eychene A. Cell context reveals a dual role for Maf in oncogenesis. Oncogene 2005;25:1299–1310. [PubMed: 16247450]
65. Kataoka K, Shioda S, Yoshitomo-Nakagawa K, Handa H, Nishizawa M. Maf and Jun nuclear oncoproteins share downstream target genes for inducing cell transformation. J Biol Chem 2001;276:36849–36856. [PubMed: 11461901]
66. Parkin SE, Baer M, Copeland TD, Schwartz RC, Johnson PF. Regulation of CCAAT/enhancer-binding protein (C/EBP) activator proteins by heterodimerization with C/EBPgamma (Ig/EBP). J Biol Chem 2002;277:23563–23572. [PubMed: 11980905]
67. Huguier S, Baguet J, Perez S, van Dam H, Castellazzi M. Transcription factor ATF2 cooperates with v-Jun to promote growth factor-independent proliferation in vitro and tumor formation in vivo. Mol Cell Biol 1998;18:7020–7029. [PubMed: 9819389]

68. Lu R, Misra V. Zhangfei: a second cellular protein interacts with herpes simplex virus accessory factor HCF in a manner similar to Luman and VP16. Nucleic Acids Res 2000;28:2446–2454. [PubMed: 10871379]

69. Ikushima S, Inukai T, Inaba T, Nimer SD, Cleveland JL, Look AT. Pivotal role for the NFIL3/E4BP4 transcription factor in interleukin 3-mediated survival of pro-Bâ€‰lymphocytes. Proc Natl Acad Sci U S A 1997;94:2609–2614. [PubMed: 9122243]

70. Doi M, Nakajima Y, Okano T, Fukada Y. Light-induced phase-delay of the chicken pineal circadian clock is associated with the induction of cE4bp4, a potential transcriptional repressor of cPer2 gene. Proc Natl Acad Sci U S A 2001;98:8089–8094. [PubMed: 11427718]

71. Lai CK, Ting LP. Transcriptional Repression of Human Hepatitis B Virus Genes by a bZIP Family Member, E4BP4. J Virol 1999;73:3197–3209. [PubMed: 10074173]

Abbreviations

ATP	adenosine triphosphate
BLAST	basic local alignment search tool
BSA	bovine serum albumin
bZIP	basic-region leucine-zipper transcription factor
CD	circular dichroism
DTT	dithiothreitol
EDTA	ethylenediaminetetraacetic acid
GdnHCl	guanidine hydrochloride
HPLC	high performance liquid chromatography
IPTG	isopropyl β-D-1-thiogalactopyranoside
MBP	maltose-binding protein
Ni-NTA	nickel-nitrilotriacetic acid
PBS	phosphate buffered saline
PAGE	polyacrylamide gel electrophoresis
PCR	polymerase chain reaction
PNK	polynucleotide kinase
TBE	tris/borate/EDTA
TEV	tobacco etch virus
TRIS	tris(hydroxymethyl)aminomethane

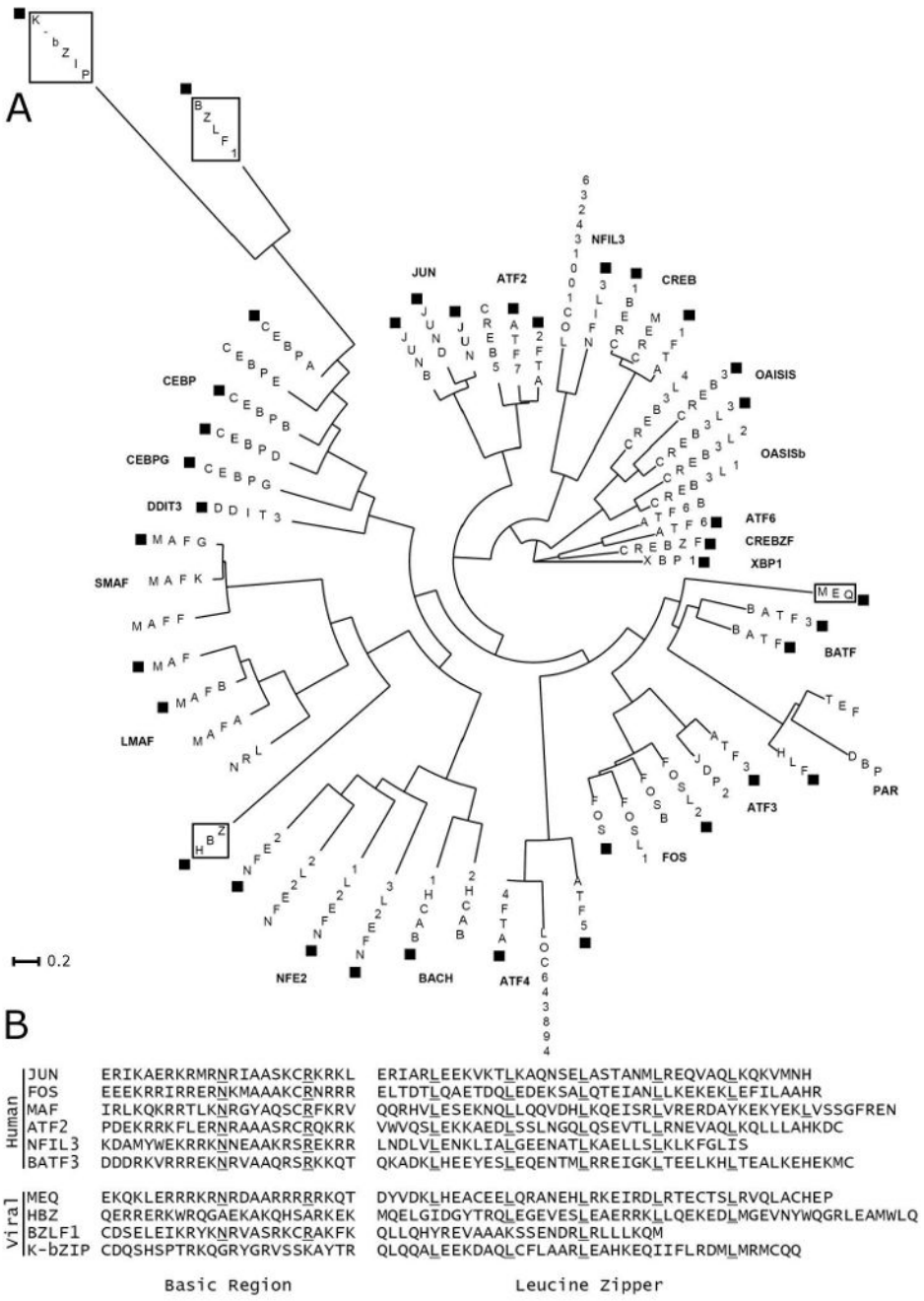

Figure 1.

Sequence properties of human and viral bZIPs. (A) A phylogenetic tree was inferred by neighbor-joining using only the leucine-zipper region of each of the 53 human bZIPs and the 4 viral bZIPs. Viral sequences are boxed. Proteins used to measure interactions are indicated with a black square. Family names are in bold. The scale bar refers to amino-acid changes per position. (B) Multiple-sequence alignment of viral bZIPs with representative human bZIPs. The following are underlined: Highly conserved basic-region asparagine and arginine residues and conserved leucines in the leucine zippers.

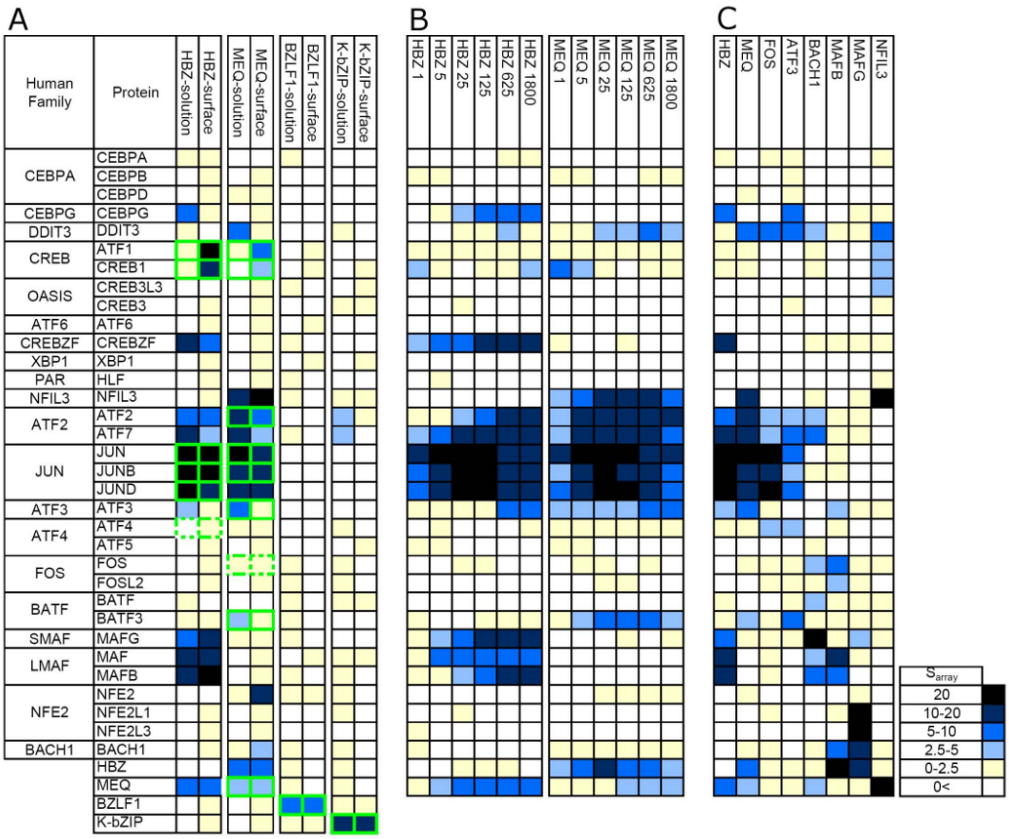

Figure 2.

Identification of viral bZIP interactions using peptide microarrays. Interactions are displayed as a color map, as indicated by the scale at right. Family names are listed in the first column and individual proteins are listed in the second column. (A) Interactions made by 4 viral proteins, when in solution or on the surface, are shown in columns. The potential interaction partners are in rows. Each heteromeric interaction is shown twice, corresponding to the two different ways it could be measured. Observations in agreement with prior studies are boxed in green; those interactions reported to be weak in the literature are indicated with dashed boxes. Fluorescently labeled proteins were used at 160 nM in a phosphate buffer that included 1M guanidine hydrochloride (GdnHCl), except BZLF1 was used at a probe concentration of 1280 nM and K-bZIP was used at a probe concentration of 640 nM in 2.2 M GdnHCl. (B) MEQ and HBZ interactions at concentrations of 1-1800 nM. (C) Interaction profiles for 6 human proteins used as solution probes are shown for comparison to HBZ and MEQ solution profiles.

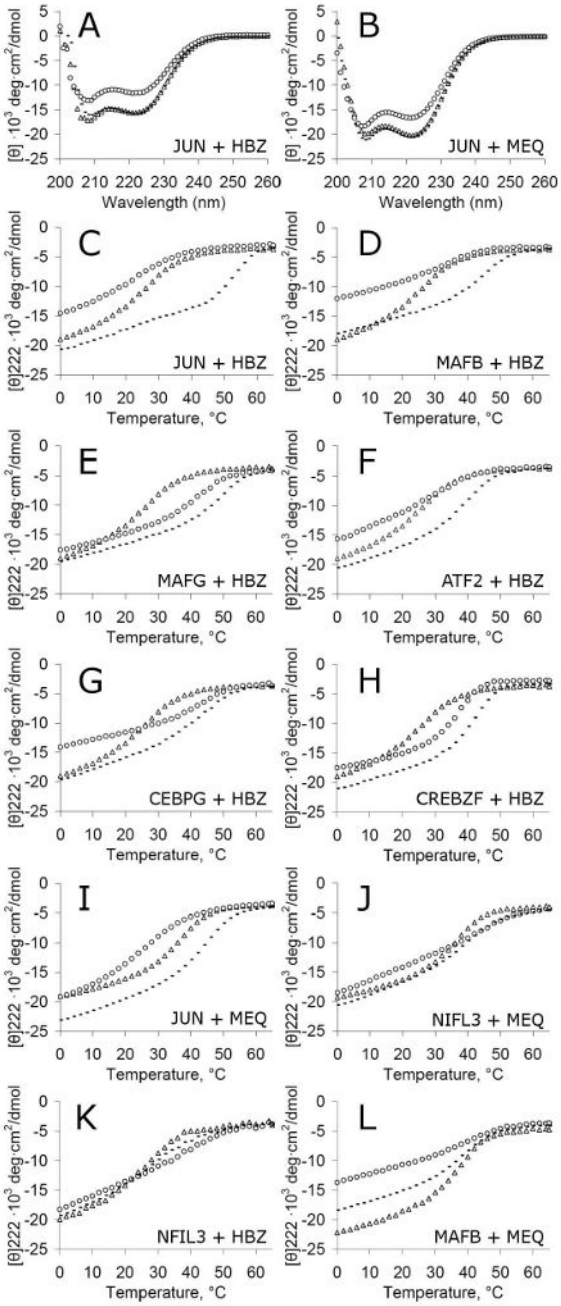

Figure 3.

Solution measurements of novel interactions for HBZ and MEQ. (A and B) CD spectra at 40 μM for each protein or 80 μM for each mixture at 25 °C. (A) HBZ (open triangles), JUN (open circles), mixture (dashed line). (B) MEQ (open triangles), JUN (open circles), mixture (dashed line). (C-L) Thermal melts monitored by CD at 4 μM for each protein or 8 μM for each mixture. All mixtures are shown in dashed lines. (C) HBZ (open triangles), JUN (open circles). (D) HBZ (open triangle), MAFB (open circles). (E) HBZ (open triangles), MAFG (open circles). (F) HBZ (open triangles), ATF2 (open circles). (G) HBZ (open triangles), CEBPG (open circles). (H) HBZ (open triangles), CREBZF (open circles). (I) MEQ (open triangles), JUN

(open circles). (J) MEQ (open triangles), NFIL3 (open circles). (K) HBZ (open triangles), NIFL3 (open circles). (L) MEQ (open triangles), MAFB (open circles).

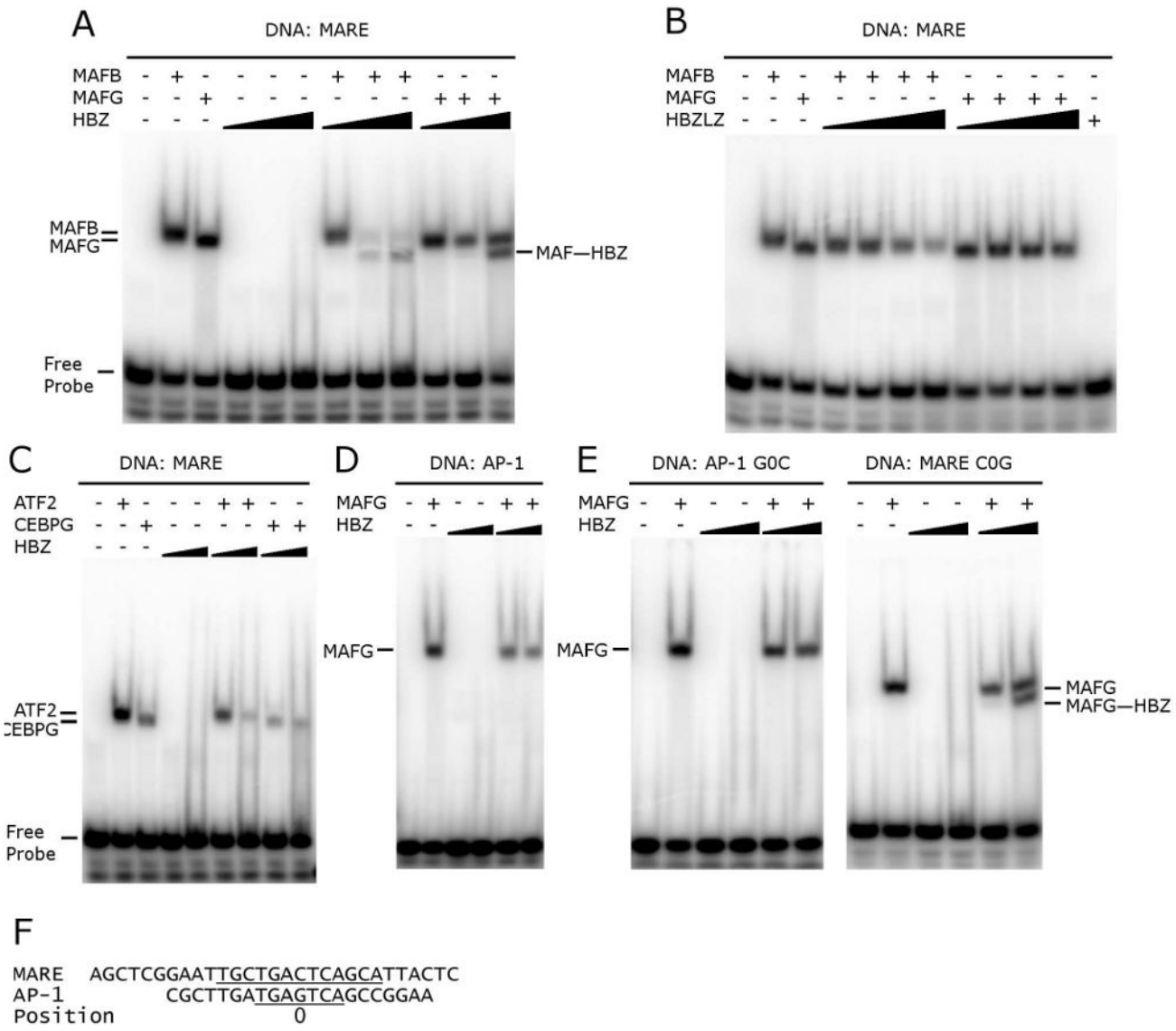

Figure 4.

Binding of HBZ and human bZIPs to specific DNA sites assessed by gel-shifts. Homo- and hetero- complexes formed on DNA are indicated. (A) HBZ can form heterocomplexes with MAFB or MAFG on MARE DNA sites. The concentration of MAFB was 4 nM, MAFG was 4 nM, and HBZ was 4, 40 or 400 nM. (B) A leucine-zipper-only version of HBZ (HBZLZ) prevents MAFB and MAFG from binding MARE-site DNA. The concentration of MAFB was 4 nM, MAFG was 4 nM, and HBZLZ was at 4, 40, 400, or 4000 nM. HBZLZ incubated alone was at 4000 nM. (C) HBZ prevents ATF2 and CEBPG from binding MARE-site DNA. The concentrations of ATF2 and CEBPG were 20 nM, and HBZ was at 40 or 400 nM. (D) HBZ prevents MAFG from binding AP-1 DNA. The concentration of MAFG was 20 nM, and HBZ was at 40 or 400 nM. (E) AP-1-site variant TGACTCA (G0C) was not sufficient for HBZ to bind DNA with MAFG. The concentration of MAFG was 20 nM with AP-1 G0C and 4 nM with MARE C0G. The concentration of HBZ was 40 or 400 nM. (F) DNA sequences used in gel-shift assays; the consensus site is underlined and position 0 is indicated.

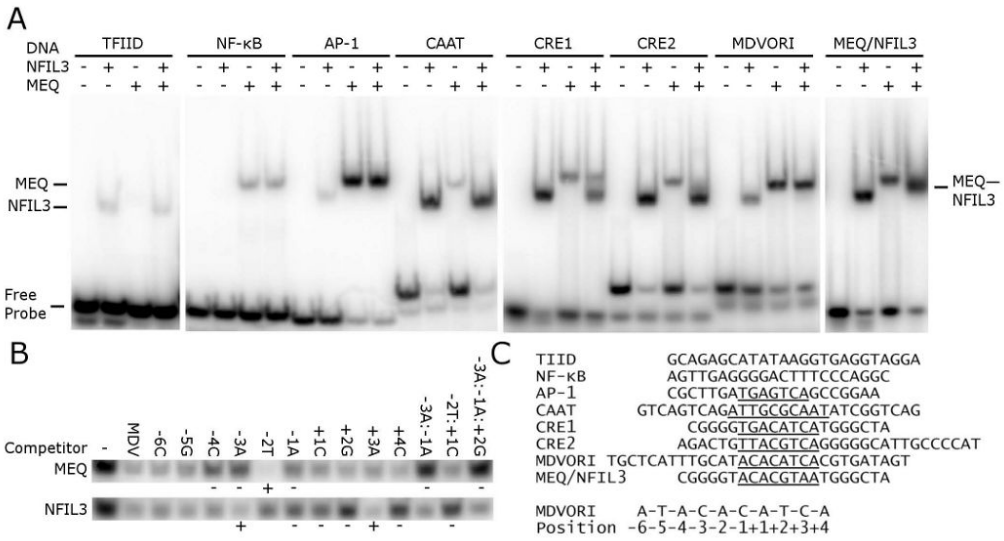

Figure 5.

MEQ and NFIL3 interact and have different but overlapping DNA-binding specificities. (A) Gel-shift experiments with MEQ and NFIL3. The concentration of MEQ and NFIL3 was 80 nM each or 160 nM total protein for mixtures. Each homodimer and heterodimer is indicated. (B) Competition gel-shift demonstrates that MEQ and NFIL3 bind to similar regions of an MDVORI probe, but have differing specificities. Each protein was at 80 nM incubated with 0.7 nM radiolabeled MDVORI DNA. Above each lane is listed the mutation or mutations made in cold competitor DNA (400 nM). Three individual experiments were quantified, and those positions that gave ≥ 2-fold changes are indicated (+/- indicate increase/decrease in binding). (C) DNA sequences used in gel-shift assays; the consensus site is underlined. The positions of the MDVORI site are numbered.

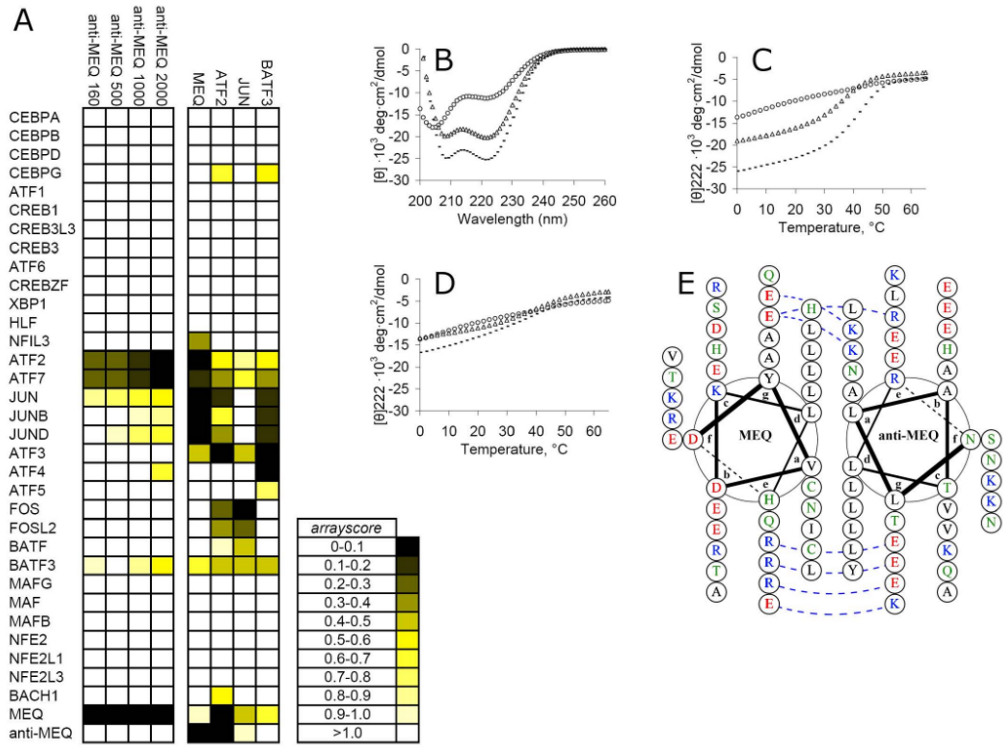

Figure 6.

Anti-MEQ binds MEQ with high affinity and specificity. (A) Designed peptide anti-MEQ characterized using coiled-coil arrays. Color map of *arrayscore* is shown, with the colors defined in the scale. Left, anti-MEQ at different concentrations (nM) in solution is listed in columns, with proteins printed on the surface in rows. Right, MEQ and 3 human bZIPs tested against anti-MEQ and other proteins printed on the surface. (B) CD spectra at 40 μM for each protein or 80 μM for the mixture taken at 25 °C. MEQ (open triangles), anti-MEQ (open circles), and the mixture (dashed line). (C and D) Thermal melts monitored by CD at 4 μM for each protein or 8 μM for the mixture. (C) MEQ (open triangles), anti-MEQ (open circles), and the mixture (dashed line). (D)ATF2 (open triangles), anti-MEQ (open circles), and the mixture (dashed line). (E) Helical wheel diagram predicted for the interaction of MEQ with anti-MEQ. The complex is depicted as a parallel dimer, and the two helices of the coiled coil are shown from the N-terminus, with the sequence read clockwise and outwards on each helix. Coiled-coil heptad positions are labeled. Hydrophobic residues are in black, charged residues are in red/blue, and polar residues are in green. Potential attractive electrostatic interactions are shown in dashed blue lines. Diagram created using DrawCoil 1.0. (http://www.gevorggrigoryan.com/drawcoil/).

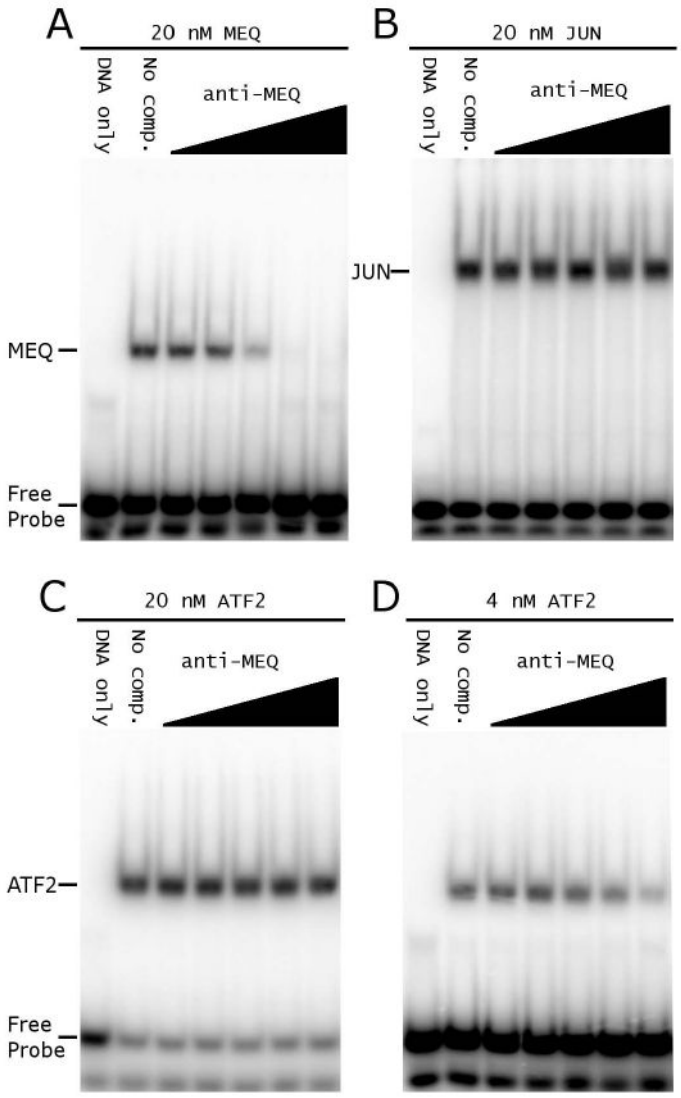

Figure 7.

Anti-MEQ prevents MEQ from binding DNA. Competition gel-shifts with a constant amount of the indicated protein bound to DNA were titrated with increasing amounts of anti-MEQ. Concentrations of competitor peptide were 0.02, 0.1, 0.5, 2.5, and 12.5 μM. Labeled DNA was present at 0.7nM. (A) 20 nM MEQ with MDVORI DNA. (B) 20 nM JUN with AP-1 DNA. (C) 20 nM ATF2 with CRE2 DNA. (D) 4 nM ATF2 with CRE2 DNA.